Deep-Learning Framework of Sea Ice Surface Roughness and Thickness Predictions Using SAR Data

By Sangwon Lim (V00923765) and Omar Kawach (V00925658)

GEOG422: Advanced Topics in Remote Sensing
Geomatics (Geography & Computer Science)
University of Victoria
Victoria, BC, Canada
Apr / 18 / 2022

Table of Contents

Abstract

In the Canadian Arctic Archipelago, melt seasons have gotten longer, overall sea ice area has decreased, and sea ice variability has increased due to climate change and human activity. It would be beneficial to explore how they affect local communities, vessels, and the environment. However, Canada's north is massive and cannot be studied on a large scale with in-situ measurements, so using remotely sensed synthetic aperture radar data would be superior. Remote sensing data could be used to create a deep learning framework for sea ice research. In this study, the proposed framework's preprocessing techniques and convolutional deep learning models must be capable of incorporating sea ice type classification, surface roughness regression, and thickness regression. The performance of the 3D convolutional neural network and 3D convolutional autoencoder models showed improvements in sea ice type classification. Speckles in the unfiltered SAR data could be leveraged to infer some sea ice characteristics. The supervised nature of the convolutional neural network outperformed the unsupervised convolutional autoencoder in sea ice type classification due to the complexity involved with extracting information from unfiltered data. Reciprocal learning between the sea ice surface roughness and thickness regression processes after many recursions showed promise in improving the performance of both processes. Sea ice features within an input image could be extracted via a streamlined approach such as shell scripting or docker containerization once the deep learning framework had been developed.

Introduction

The Canadian Arctic Archipelago (CAA), like much of the global arctic, has been threatened by climate change and human activities for decades. Consequently, melt seasons have gotten longer, overall sea ice area has decreased, and sea ice variability has increased (Howell et al., 2009). More than locals, researchers, and vessels may be impacted as a result of the threats the CAA faces. The marine ecosystem of CAA, for example, is a massive hub of benthic biodiversity (Wei et al., 2020). Freshwater discharge, which has become more common in the arctic (Syed et al., 2007), has the potential to harm the diversity and functions of benthic communities (McGovern et al., 2020). Given the large landmass of the CAA, using satellite imagery to support sea ice navigation, arctic communities, researchers, and biodiversity may be a viable option for change detection, unlike in-situ measurements.

In literature, synthetic aperture radar (SAR) remote sensing for sea ice research has been well established. There are numerous advantages to using SAR remote sensing data. Applications such as change detection of sea ice require temporal coverage, surface characterization, and day and/or night observations without noise from the climate (Barber et al., 2001). SAR's active microwave sensor(s) and available data quality may meet these requirements. However, having data is not enough to characterize the sea ice surfaces. Further processing is necessary. Advanced technologies, such as machine learning, may overcome the difficulty of ice surface characterization (Blix & Eltoft, 2021). Therefore, models to predict sea ice roughness and thickness must be developed using SAR data.

According to Von Saldern et al. (2006), the surface roughness parameters of the mean profile height, standard deviation of the profile elevation about the mean (rms height) and fractal dimension showed significantly strong correlations with the thickness. Moreover, the parameterization enhanced the performance in detecting thick First-Year Ice (FYI) and Old-Ice, which comprises Second-Year Ice Multi-Year Ice (MYI). From the evidence showing the correlations between sea ice features (surface roughness, thickness and type), this study proposes a deep learning framework that aims to reciprocally enhance each feature’s prediction.

In addition to the discussion of the framework, a comparative experiment is performed to assess whether speckle filtering of SAR data is advantageous when applied to deep learning. Speckle filtering has been emphasized by multiple studies since they are considered noise caused by coherent constructive or destructive interference in backscattered waves (Dasari et al., 2015; Lee et al., 1994). However, the salt-and-pepper noise may infer the surface complexity information of the scatterer, which is anticipated to be extracted using convolutional deep learning.

Study Area and Data

Study Area

The area of interest for this study is the CAA. The CAA covers about 10% of Canada's landmass and is located in the country's northern region. Large ice caps occupy many of the CAA's

major and minor islands (Adams & Dunbar, 2015), making them ideal for sea ice research. This study will focus on data from voyages through Victoria Island, Prince of Wales Island, Somerset Island, and King William Island in 2015, 2016, and 2018. (see Figure 1).

Figure 1. Map of Canadian Arctic Archipelago with Inset

SAR Data

RADARSAT-2 data retrieved with ScanSAR Wide mode with horizontal transmit and horizontal receive (HH), and horizontal transmit and vertical receive (HV) polarization bands are used for the study. A fine spatial resolution of 50 meters range and azimuth spacing enhances the project's practicality. Incident angle (IA) data are assigned per pixel. The images were collected from March to April in 2015, 2016 and 2018 with about 7-day temporal resolution. The low-level data are only geo-rectified without speckle filtering processes.

Expert Data

Sea ice surface roughness and thickness data were collected from an airborne electromagnetic (AEM) platform on April 19, 2015, April 8, 2016, and May 8, 2018. Data points are linearly distributed along the flight lines with ~1.2 m and ~5.5 m intervals for surface roughness and thickness. The surface roughness parameter used is rms, and thickness values are in meters. Each data point is assigned longitude and latitude coordinates. Sea ice type data for the corresponding dates are provided by a professional sea ice expert. Pixels are labelled as FYI, Deformed FYI (DFYI) and MYI.

Methods

Data Selection and Preprocessing

RADARSAT-2 images collected around the dates of AEM data collection are selected for the study: April 18, 2015, April 19, 2015, April 9, 2016, April 10, 2019, April 29, 2018, and April 30, 2018. The last image of each year, with the last date and time of data collection, is separated for creating test datasets, while the rest are used to train deep learning models.

The SAR images are speckled filtered using the Sentinel Application Platform (SNAP) software (European Space Agency, 2020; Faizan, 2020) to experiment with the effectiveness of using the processed data in deep learning for sea ice applications. Boxcar filtering with a 7x7 sliding window is performed. IA layers are extracted using the same software tool. One of the main objectives of data processing is to link the AEM data points with pixels in the SAR images. SNAP was used again to accomplish the objective. However, the number of samples processed at once is limited, and many expert data points must be removed. As a result, two AEM points fall in a pixel at most. If two points are in a pixel, they are averaged to assign a label to the sample.

Both surface roughness and thickness data are right-skewed, with lesser occurrences in greater values (Figure 2). The one-sided selection undersampling method with 25 equal-interval bins was used to mitigate the effect of overfitting from overly clustered labels. Moreover, log transformation with the natural logarithm function is applied to the values to train models in a gaussian distribution. Random oversampling is performed to match the number of samples in each class before sea ice type classification.

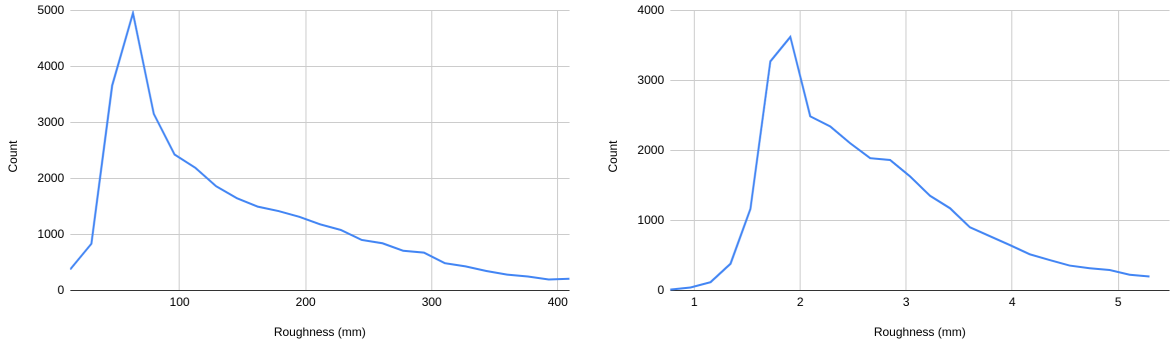

Figure 2. Histograms of surface roughness (left) and thickness data (right).

Deep Learning Framework

The study proposes a deep learning framework incorporating sea ice type classification, surface roughness regression and thickness regression (Figure 3). The first process, sea ice type classification, outputs the likelihoods of FYI, DFYI and MYI, adding up to 1. The values are concatenated as features to further processes of surface roughness and thickness regressions. The two processes are reciprocally connected in a Residual Network (ResNet) by recursively feeding surface roughness or thickness prediction results to each other in an interleaving order, which accomplishes both forward and backward propagations. The design is based on the hypothesis that both features

have positive impacts on enhancing performances. The ResNet is anticipated to improve the performances with multiple recursions.

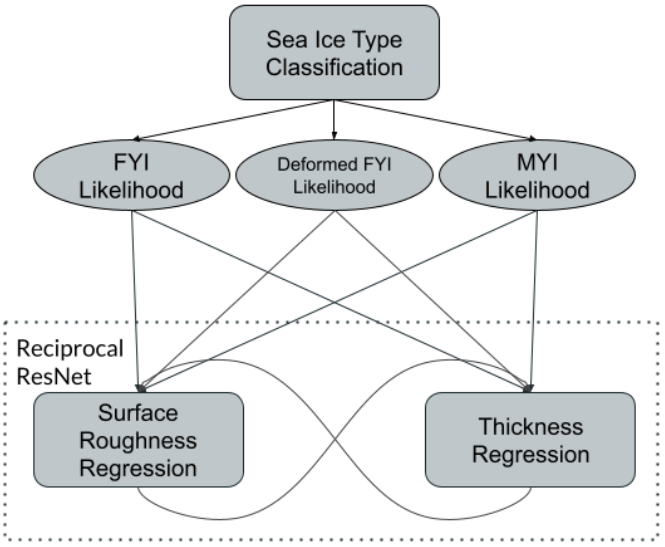

Figure 3. Deep learning framework of sea ice surface roughness and thickness predictions

Convolutional Deep Learning Architectures

Convolutional deep learning is widely used in the fields of computer vision and remote sensing, and it has shown effectiveness in sea ice applications using active microwave data (Boulze et al., 2020). It takes advantage of neighbouring pixels and extracts features without human bias or interpretations through fast computation. Two different architectures, Convolutional Autoencoder (CAE) and Convolutional Neural Network, taking 3D inputs of three 7x7 sliding window layers of HH, HV and IA, are designed for this study. Both speckle-filtered and unfiltered data are experimented with using the architectures.

3D-CAE consists of encoding and decoding processes, and its main purpose is to preserve most information in a reduced number of features (Figure 4). Therefore, the training in the architecture focuses on reverting the layer stack to the original input through both encoding and decoding. The unsupervised learning is not provided with expert data, so the encoded data contains the information that statistically explains the original input rather than the target objectives of sea ice type, surface roughness and thickness. After the training, the encoded features are concatenated with backscattering features of raw HH, speckle-filtered HH, raw HV, speckle-filtered HV and IA. The concatenation layer is then fed into a multi-layer neural network with five hidden layers. Loss functions of Categorical Crossentropy and Squared Mean Error (MSE) are used for classification and regression problems, respectively. MSE emphasizes errors in low or high values, which can mitigate the problems that underrepresented data might entail.

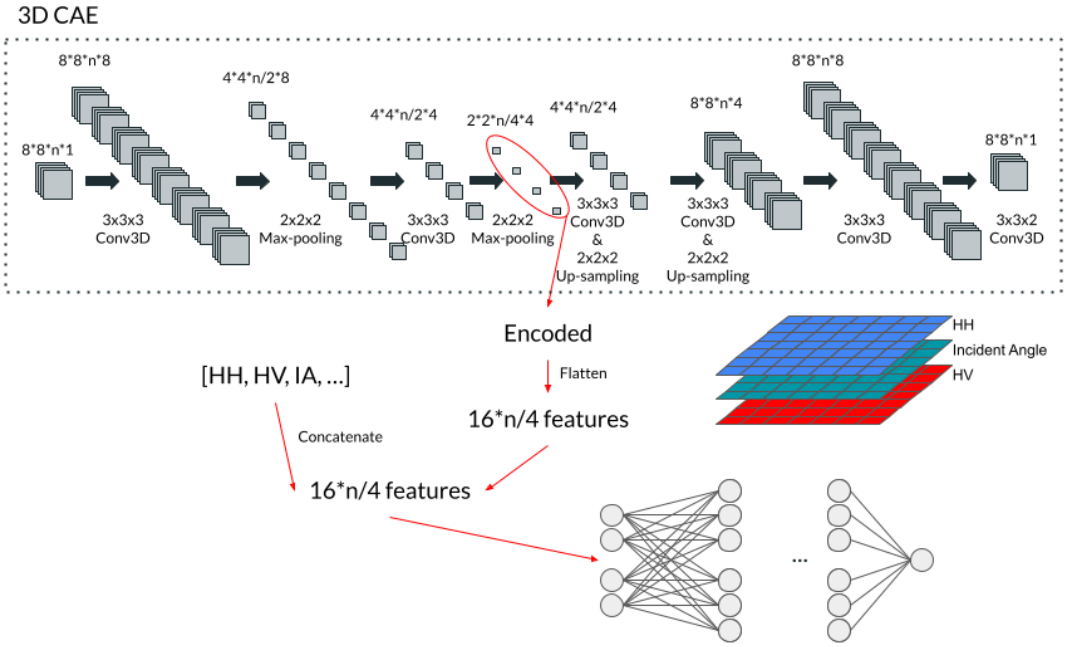

Figure 4. Illustration of 3D Convolutional Autoencoder. The encoding and decoding processes are performed within the dotted boundary.

The 3D-CNN architecture resembles the encoding part of 3D-CAE but is trained in a supervised manner where the expert target labels are provided (Figure 5). Therefore, the output models likely fit into the objectives better than the autoencoder but may lose some unknown information that the layer-stacks have. The concatenation of backscattering features followed by a multilayer neural network is also applied in 3D-CNN.

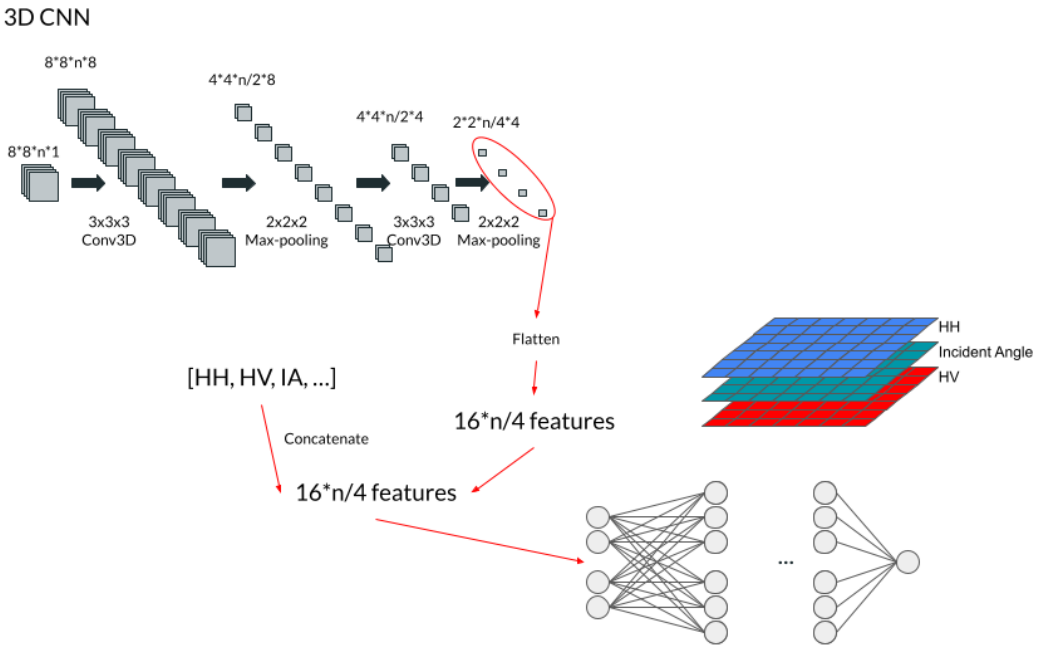

Figure 5. Illustration of 3D Convolutional Neural Network.

Performance Assessment

The accuracy of sea ice type classification is defined by the ratios of accurately predicted samples in FYI, DFYI and MYI classes. Confusion matrices are effective for the visualization of classification performances. Three metrics, Mean Absolute Error (MAE), Root Mean Squared Error (RMSE) and R^2 score, are used for assessing regression problems (Equations 1, 2 and 3). The MAE is the most intuitive metric showing how much the predictions are different from real values. The RMSE has the same effect as the MSE to emphasize the underrepresented values. R^2 scores indicate how much the predictions are well distributed while accomplishing a good performance. Lower MAEs and RMSEs, and higher R^2 scores indicate better regression performances.

$$MAE = \frac{|predicted - expert|}{N} \quad \text{(Equation 1)}$$

$$RMSE = \sqrt{\frac{\Sigma(predicted - expert)^2}{N}} \quad \text{(Equation 2)}$$

$$R^2 = 1 - \frac{\Sigma(predicted - expert)^2}{variance(prediction)} \quad \text{(Equation 3)}$$

Where N = number of samples

Streamlining of Sea Ice Feature Extractions

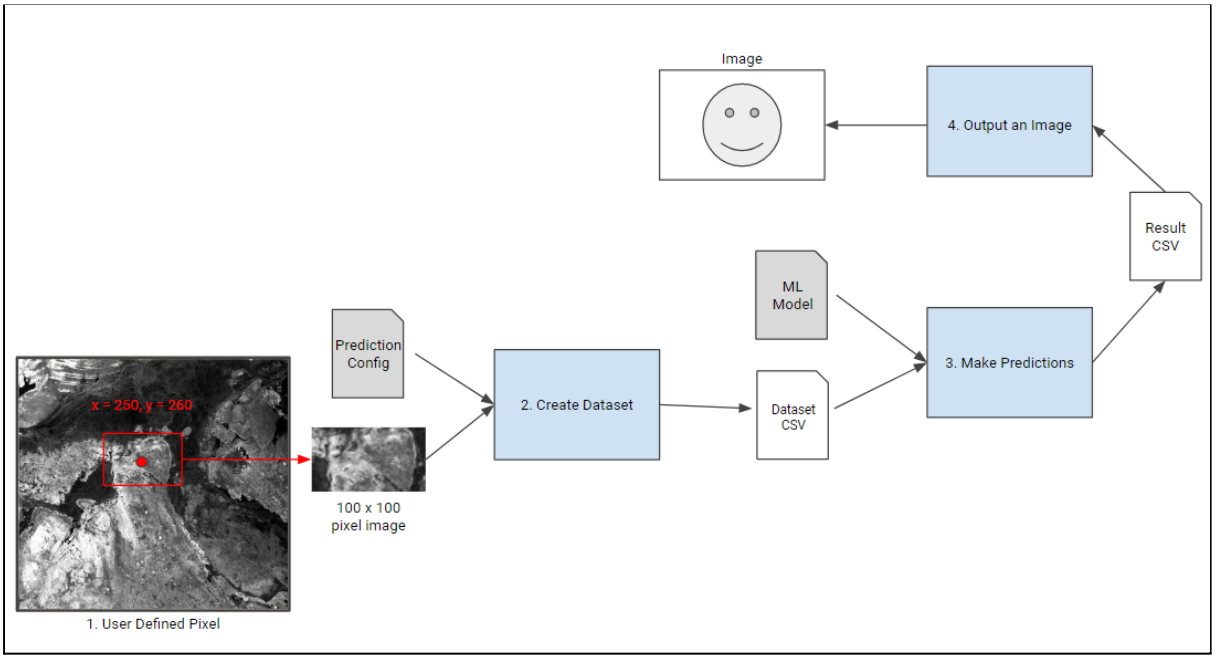

Figure 5. The 4 Sea Ice Classification Processes that are Streamlined

The processes stated above must be connected using streamlining in order to take advantage of the deep learning framework developed for the sea ice classification and regressions. There are four processes to go from an unclassified input image to an output image. Because the photos are fairly large (> 1 gigabyte), the first process is to identify a user-defined 100 × 100 pixel of interest inside the input image. Then, to construct feature vector datasets, configuration files take in parameters such as the pixel of interest. Machine learning models use these vector datasets in order to predict sea ice

type, roughness, and thickness. Finally, the prediction's output dataset is turned into an output image. Using a simple script (e.g., shell script) or containerization (e.g., docker), these four processes can be piped together into a single process. Users only have to specify their input image once, define a 100 × 100 pixel somewhere in the input image, and then leave the rest to the script or container.

Results

Sea Ice Type Classification

Classification of FYI, DFYI and MYI was performed using different architecture and feature combinations (Figure 7). Results using a simple multi-layer neural network with backscattering features of HH, speckle-filtered HH, HV, speckle-filtered HV and IA work as the baseline at about 55.59% on average (σ=0.088) in the K-fold (K=10) validation. The degradation of the performance is mainly driven by low accuracies in DFYI classification (μ=13.96%) where the models greatly confused the class with MYI. Using 3D-CNN or 3D-CAE architectures mitigates this confusion and improved the average performance by ~11.4% to ~16.5%. 3D-CNN produced better results using unfiltered data (μ=72.05%; σ=0.041), while better 3D-CAE results were generated using speckle-filtered data (μ=71.52%; σ=0.048). Concatenating the two architectures reduced the standard deviation in the validated results (μ=71.57%; σ=0.023), indicating more reliable models. The best accuracy attained using the concatenation of 3D-CNN and 3D-CAE architectures is 74.16% (Figure 8).

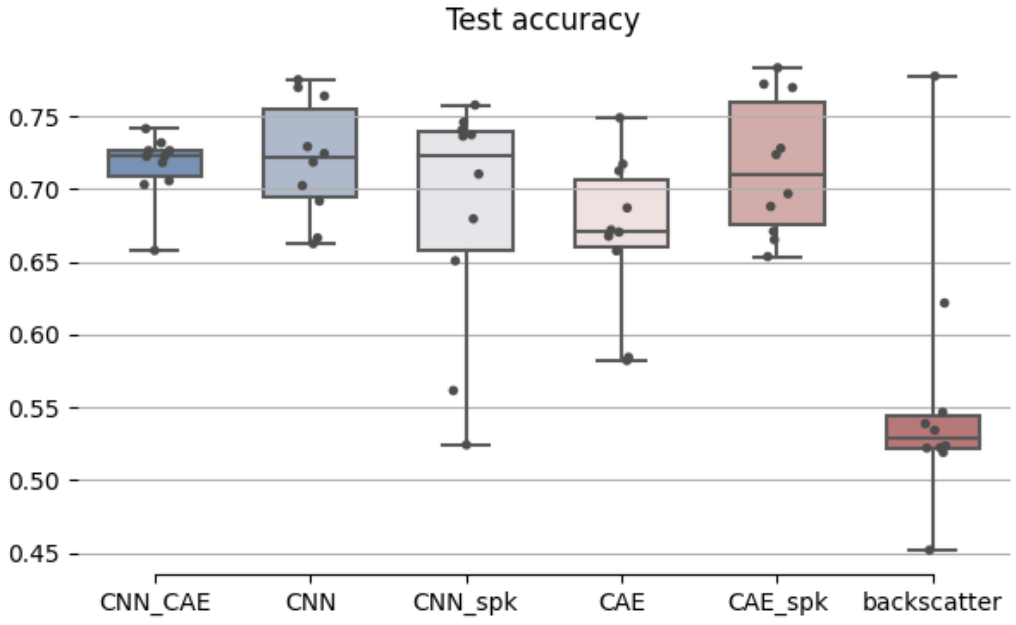

Figure 7. Box plot showing the K-fold (K=10) validation results of sea ice type classification.

Figure 8. Confusion matrix of the best test result obtained using the concatenation of 3D-CNN and 3D-CAE architecture (0=FYI; 1=DFYI; 2=MYI).

Sea Ice Surface Roughness and Thickness Regressions

The classification results suggest the concatenation of 3D-CNN with unfiltered data, CAE with speckle filtered data, and backscattering features altogether as a good practice. The best classification model generated was used to enhance the sea ice surface roughness and thickness regressions. When compared with the standalone processes, feeding likelihoods of FYI, DFYI and MYI from classification showed improvement in sea ice surface roughness and thickness regressions in every metric except for the R^2 score in surface roughness and RMSE in thickness predictions (Figure 9). One apparent characteristic in the prediction results enhanced using likelihood features is that there are two clusterings in the scatter plots at lower and higher prediction values (Figure 10).

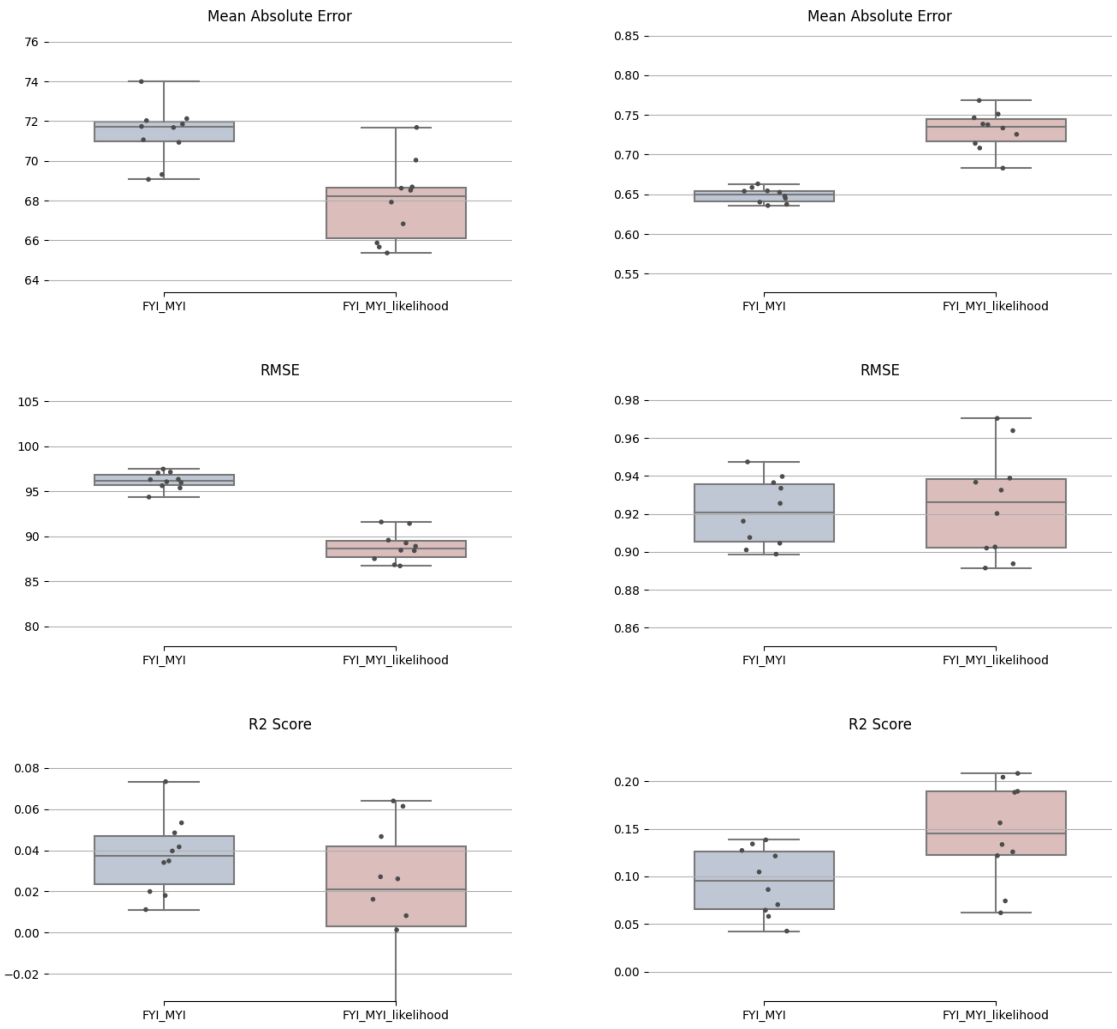

Figure 9. Box plots showing the K-fold (K=10) validation results of sea ice surface roughness (left) and thickness (right) regressions in three metrics (top=MAE; middle=RMSE; bottom=R^2).

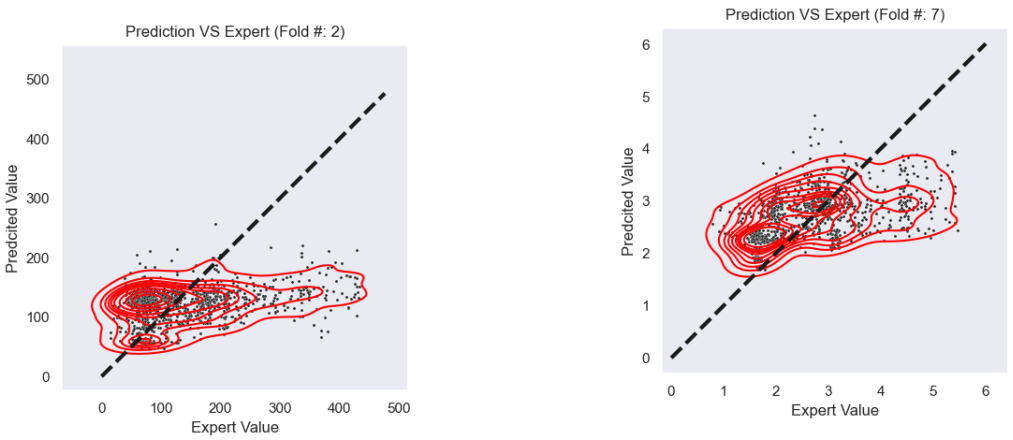

Figure 10. Scatter plots with the best RMSE results in sea ice surface roughness and thickness predictions enhanced using sea ice type likelihood features.

Fifty recursions are performed in the reciprocal ResNet to enhance surface roughness and thickness regressions (Figure 11). Multiple dips spikes of MAE, RMSE and R^2 score are observed in the recursion logs. ResNet improves both surface roughness (MAE=56.77mm; RMSE=78.99mm) and thickness results (MAE=0.48; RMSE=0.73m) (Figure 12). Two clusterings in the predictions still occur in scatter plots, but the results show a higher density near the diagonal (Expert Value = Prediction Value) line (Figure 13). The models are incapable of predicting surface roughness and thickness values higher than 200mm and 3.5m, respectively.

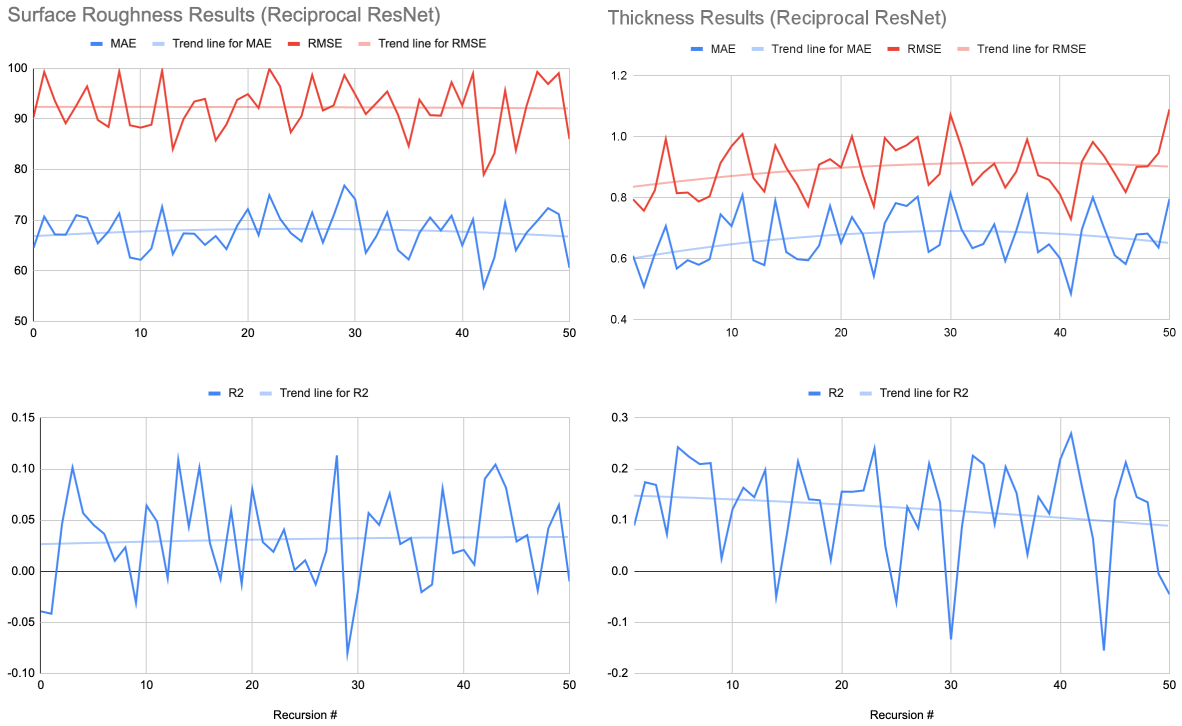

Figure 11. Log of MAE, RMSE and R^2 score of surface roughness (left) and thickness (right) regressions through fifty recursions in the reciprocal ResNet.

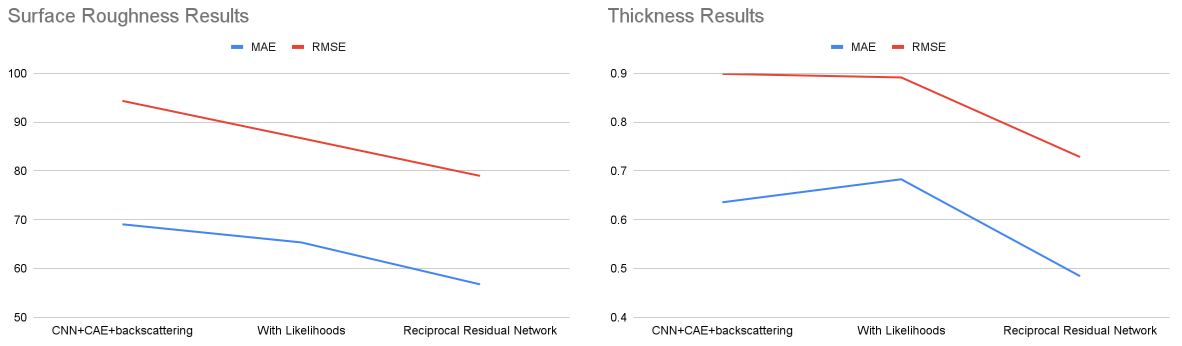

Figure 12. Minimum MAE and RMSE comparisons between the methods of standalone training, enhancement using sea ice type likelihoods and enhancement from reciprocal ResNet.

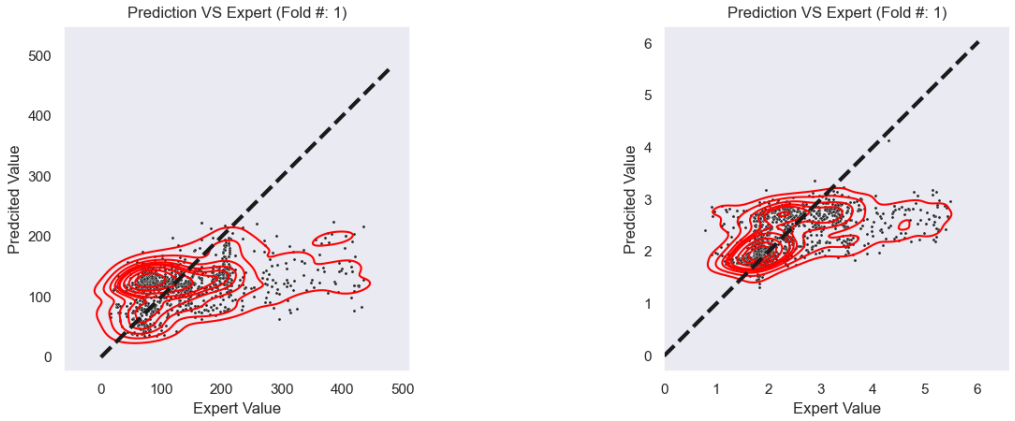

Figure 13. Scatter plots with the best RMSE results in sea ice surface roughness and thickness predictions enhanced from reciprocal ResNet.

Streamlining Outputs

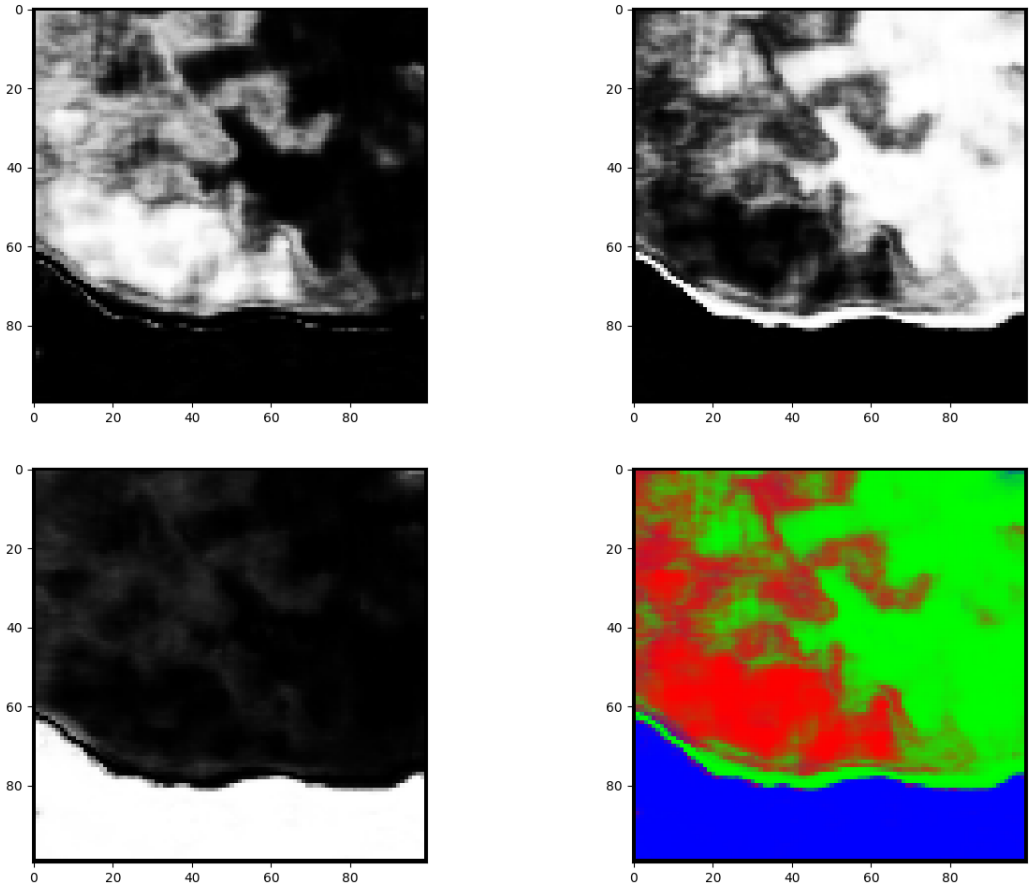

Figure 14. Sea ice type classification of 100x100 image around 70°40'N 102°22'W: FYI likelihood map (left-top), DFYI likelihood map (right-top), MYI likelihood map (left-bottom) and RGB composite map (right-bottom; Red=FYI; Green=DFYI; Blue=MYI).

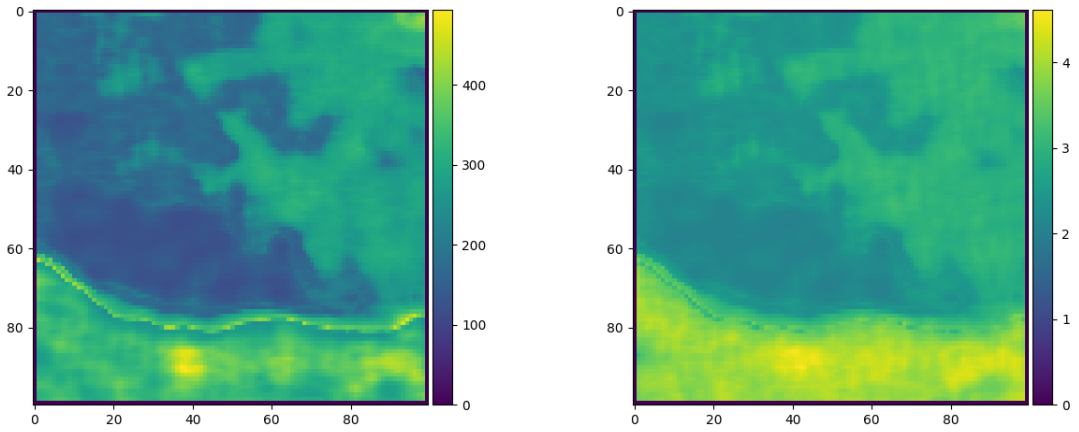

Figure 15. Sea ice surface roughness (left) and thickness (right) predictions of 100x100 images around 70°40'N 102°22'W.

Sea ice type classification and surface roughness/thickness regression outputs at a location in CAA are produced using streamlining (Figures 14 and 15). The 100x100 pixels cover a 25km^2 area with great variability in the SAR backscattering and AEM data. All FYI, DFYI and MYI classes are distributed in the region (Figure 14). The surface roughness and thickness prediction outputs visualize a similar distribution as the classification outputs, where FYI, DFYI and MYI have low, medium and high values, respectively.

Discussion

The experiments with convolutional deep learning for sea ice type classification indicate that both 3D-CNN and 3D-CAE improve the performance but with different significance levels. 3D-CNN models performing better than 3D-CAE using unfiltered data suggest that supervised learning provided with the direction of expert data is better than letting unsupervised architecture train itself to extract important information. However, because of the versatility of unsupervised learning, 3D-CAE may still be used to assist 3D-CNN architectures by adding information that might have been ignored. The 3D-CNN architecture benefitted from unfiltered SAR data, suggesting that some sea ice characteristics can be inferred from speckles. In contrast, 3D-CAE performed better with speckle-filtered data, but it is assumed that encoding and decoding performance depends on the complexity of preserving information from input images. More homogeneous images are likely better encoded than the ones with hard-to-predict salt-and-pepper noise.

The first step of the deep learning framework, feeding sea ice type likelihoods to surface roughness and thickness predictions, successfully enhanced the performances. However, the two clusterings in regression results are assumed to be caused by older ice relating to rougher and thicker ice (Von Saldern et al., 2006), and deep learning was able to detect the relationships. Such a behaviour of the models relies significantly on the sea ice type classification causing unnatural predictions.

Reciprocal ResNet devised for this project seems to mitigate the effect while also accomplishing performance enhancements.

The output images of sea ice type, surface roughness and thickness show strong correlations between each other, where they share a similar spatial distribution. It proves the hypothesis that connecting all three processes can potentially benefit each other. Thus, the design of the deep learning framework and reciprocal ResNet suggested in this study are logically backed with evidence along with the previous study by Von Saldern et al. (2006).

Additionally, models are observed to be incapable of predicting higher values for both surface roughness and thickness predictions. This will require thresholding of predicted values where some samples should be simply classified as very rough or thick sea ice instead of fitting into numeric values. Due to the expensive computational cost of the architecture, only fifty recursions were performed, but the improving trends in the MAE, RMSE and R^2 still persisted.

Conclusion

The promising results of the proposed deep learning framework suggest that using 3D-CAE and 3D-CNN architectures for sea ice research may be a viable application. However, there is room for improvement. Future work may benefit from the use of fast parallel computing to test whether performance can be enhanced by doing many more recursions. The streamlined approach to sea ice feature extraction abstracts away the complex processes involved. Since no knowledge of the architecture or code is necessary to produce an output from an image, this level of abstraction may be sufficient for making the framework available to subject matter experts in the future.

Acknowledgements

This study would not be possible without Dr. Randy Scharien's provision of the expert data and teaching the Advanced Topics in Remote Sensing course at the University of Victoria. Aikaterini Tavri, the teaching assistant, played a huge role in providing insights into SAR data processing. Additionally, the RADARSAT-2 data provided by the Canadian Space Agency was an essential requirement of the project. The interdisciplinary program combining Computer Science and Geography at University of Victoria allowed the authors to have a meaningful chance to conduct the research. They are grateful to attain the degree with such a closure.

References

Adams, P., & Dunbar, M. (2015). Arctic Archipelago. In The Canadian Encyclopedia. Retrieved from https://www.thecanadianencyclopedia.ca/en/article/arctic-archipelago

Barber, D. G., Hanesiak, J. M., & Yackel, J. J. (2001). Sea ice, RADARSAT-1 and arctic climate processes: A review and update. *Canadian Journal of Remote Sensing*, *27*(1), 51-61. https://doi.org/10.1080/07038992.2001.10854919

Blix, K., Espeseth, M. M., & Eltoft, T. (2021). Machine learning for arctic sea ice physical properties estimation using dual-polarimetric SAR data. *IEEE Transactions on Geoscience and Remote Sensing*, *59*(6), 4618-4634. https://doi.org/10.1109/TGRS.2020.3022461

Boulze, H., Korosov, A., & Brajard, J. (2020). Classification of sea ice types in Sentinel-1 SAR data using convolutional neural networks. *Remote Sensing*, *12*(13), 2165.

Dasari, K., Anjaneyulu, L., Jayasri, P. V., & Prasad, A. V. V. (2015, December). Importance of speckle filtering in image classification of SAR data. In *2015 International Conference on Microwave*, *Optical and Communication Engineering (ICMOCE)* (pp. 349-352). IEEE.

European Space Agency. (2020). Sentinel Application Platform (Version 8.0.0). *Science Toolbox Exploitation Platform*. Retrieved from https://step.esa.int/main/download/snap-download/.

Faizan, Mohammed. (2020). Radarsat-2 data processing using SNAP software. 10.13140/RG.2.2.33003.46881.

Howell, S. E. L., Duguay, C. R., & Markus, T. (2009). Sea ice conditions and melt season duration variability within the canadian arctic archipelago: 1979–2008. *Geophysical Research Letters*, *36*(10), L10502-n/a. https://doi.org/10.1029/2009GL037681

Lee, J. S., Jurkevich, L., Dewaele, P., Wambacq, P., & Oosterlinck, A. (1994). Speckle filtering of synthetic aperture radar images: A review. *Remote sensing reviews*, *8*(4), 313-340.

McGovern, M., Poste, A. E., Oug, E., Renaud, P. E., & Trannum, H. C. (2020). Riverine impacts on benthic biodiversity and functional traits: A comparison of two sub-arctic fjords. Estuarine, *Coastal and Shelf Science*, *240*, 106774. https://doi.org/10.1016/j.ecss.2020.106774

Syed, T. H., Famiglietti, J. S., Zlotnicki, V., & Rodell, M. (2007). Contemporary estimates of pan-arctic freshwater discharge from GRACE and reanalysis. *Geophysical Research Letters*, *34*(19), L19404-n/a. https://doi.org/10.1029/2007GL031254

Von Saldern, C., Haas, C., & Dierking, W. (2006). Parameterization of Arctic sea-ice surface roughness for application in ice type classification. *Annals of glaciology*, *44*, 224-230.

Wei, C., Cusson, M., Archambault, P., Belley, R., Brown, T., Burd, B. J., Edinger, E., Kenchington, E., Gilkinson, K., Lawton, P., Link, H., Ramey‐Balci, P. A., Scrosati, R. A., Snelgrove, P. V. R., & Burns, K. C. (2020). Seafloor biodiversity of canada's three oceans: Patterns, hotspots and potential drivers. *Diversity & Distributions*, *26*(2), 226-241. https://doi.org/10.1111/ddi.13013